Quantification of plasmodesmatal endoplasmic reticulum coupling between sieve elements and companion cells using fluorescence redistribution after photobleaching

Quantification of Plasmodesmatal Endoplasmic Reticulum Coupling between Sieve Elements and Companion Cells Using Fluorescence Redistribution after Photobleaching[1][W]

Helle J. Martens, Alison G. Roberts[2], Karl J. Oparka[3], and Alexander Schulz*

Department of Plant Biology, Royal Veterinary and Agricultural University, DK–1871 Frederiksberg C, Denmark

Transgenic tobacco (*Nicotiana tabacum*) was studied to localize the activity of phloem loading during development and to establish whether the endoplasmic reticulum (ER) of the companion cell (CC) and the sieve element (SE) reticulum is continuous by using a *SUC2* promoter-green fluorescent protein (GFP) construct targeted to the CC-ER. Expression of GFP marked the collection phloem in source leaves and cotyledons as expected, but also the transport phloem in stems, petioles, midveins of sink leaves, nonphotosynthetic flower parts, roots, and newly germinated seedlings, suggesting that sucrose retrieval along the pathway is an integral component of phloem function. GFP fluorescence was limited to CCs where it was visualized as a well-developed ER network in close proximity to the plasma membrane. ER coupling between CC and SEs was tested in wild-type tobacco using an ER-specific fluorochrome and fluorescence redistribution after photobleaching (FRAP), and showed that the ER is continuous via pore-plasmodesma units. ER coupling between CC and SE was quantified by determining the mobile fraction and half-life of fluorescence redistribution and compared with that of other cell types. In all tissues, fluorescence recovered slowly when it was rate limited by plasmodesmata, contrasting with fast intracellular FRAP. FRAP was unaffected by treatment with cytochalasin D. The highest degree of ER coupling was measured between CC and SE. Intimate ER coupling is consistent with a possible role for ER in membrane protein and signal exchange between CC and SE. However, a complete lack of GFP transfer between CC and SE indicated that the intraluminal pore-plasmodesma contact has a size exclusion limit below 27 kD.

The endoplasmic reticulum (ER) is a complex membrane system with branching tubules and flattened sacs that extends throughout the cytoplasm. As a part of the endomembrane system, the ER is responsible for the synthesis, processing, and sorting of proteins and lipids and for the regulation of cytosolic calcium levels (Staehelin, 1997; Voeltz et al., 2002). The ER is moreover an integral component of plasmodesmata in higher plants and forms the desmotubule linking the ER of neighboring cells (Roberts, 2005). Thus, plasmodesmata offer two potential pathways for transport between cells, the cytoplasmic sleeve for cytosolic solutes and the desmotubule for ER-associated molecules, respectively (Schulz, 1999). Whereas the exchange of solutes and macromolecules through the cytoplasmic sleeve is well established, information regarding the transfer of ER-associated molecules is very limited, even though some (e.g. calcium ions) might be of high significance for coordinated defense and wound responses. Transport of small solutes through the desmotubule has been demonstrated for trichome and epidermis cells using endocytotic uptake and microinjection of fluorochromes, respectively (Lazzaro and Thomson, 1996; Cantrill et al., 1999). However, green fluorescent protein (GFP) targeted to the ER lumen of epidermal cells did not move out of the transfected cell (Crawford and Zambryski, 2000). For the intercellular transport of membrane-bound molecules, the lipid bilayer comprising the desmotubule is available, whereas the plasma membrane is not (Grabski et al., 1993; Schulz, 1999).

Pore-plasmodesma units (PPUs) between sieve elements (SEs) and companion cells (CCs) take part in phloem loading in source leaves. PPUs are also involved in maintenance of essential functions in SEs throughout the entire plant (Oparka and Turgeon, 1999; Schulz, 2005). The cytoplasmic sleeve of PPUs has a large size exclusion limit, as indicated by transport of 36- to 67-kD GFP fusion proteins (Stadler et al., 2005), and shows high conductance even in early stages of differentiation (van Bel and van Rijen, 1994). Although published electron micrographs of PPUs always

[1] This work was supported by the Danish Research Council and the Danish Biotechnology Instrument Center.

[2] Present address: Cell Communication Programme, Scottish Crop Research Institute, Invergowrie, Dundee DD2 5DA, UK.

[3] Present address: School of Biological Sciences, University of Edinburgh, Mayfield Road, Edinburgh EH9 3JR, UK.

* Corresponding author; e-mail als@kvl.dk; fax 45–3528–3365.

The author responsible for distribution of materials integral to the findings presented in this article in accordance with the policy described in the Instructions for Authors (www.plantphysiol.org) is: Alexander Schulz (als@kvl.dk).

[W] The online version of this article contains Web-only data.

www.plantphysiol.org/cgi/doi/10.1104/pp.106.085803

show a desmotubular structure in PPUs, it is not clear whether this structure is continuous between the ER of the CC and the neighboring SE reticulum (SER) found only in mature SE (Sjolund and Shih, 1983). Specialization of SE as a low-resistance conduit for assimilates involves selective autophagy of the cytoplasm. Of all organelles, only the modified ER system (SER), mitochondria, and plastids persist (Sjölund, 1997; Schulz, 1998). The SER is initially present as rough ER and, at later stages, at the time of autophagy, is reshaped into stacks or convoluted tubules of reticulated smooth ER (Sjolund and Shih, 1983).

In gymnosperms, the SER may function in translocation because it has been shown to form prominent complexes on either side of sieve areas in living phloem, visualized using the ER-specific fluorochrome 3,3′-dihexyloxacarbocyanine iodide ($DiOC_6$; Schulz, 1992). In mature angiosperms, the SER typically forms a fenestrated sheet close to the plasma membrane along the lateral walls (Sjolund and Shih, 1983). The function of the SER is not fully understood, although it has been implicated as a calcium store and as a barrier between the peripheral, more stationary, part of the SE cytoplasm and the streaming phloem sap (Sjölund, 1997). Regardless of function, the parietal SER layer might well be linked via the PPUs to the ER of the CC (Oparka and Turgeon, 1999), which could be important for a range of functions, including calcium homeostasis within the SE, signaling between SEs and CCs, and posttranslational movement of Suc transporter proteins from the CC (where they are expressed) into the SE plasma membrane of Solanaceae (see Kühn et al., 1997). However, unequivocal evidence for functional coupling between the ER of CCs and SEs is lacking.

In a previous study (Wright et al., 2003), a noninvasive GFP reporter system was used to study the function of different vein classes in developing tobacco (*Nicotiana tabacum*) leaves in relation to the activity of the Suc transport protein promoter, *AtSUC2.* Using a construct in which GFP was targeted to the ER lumen, those CCs involved in phloem loading could be detected. Targeting to the ER prevented the export of the reporter into the sieve tube and its subsequent spread and unloading (Imlau et al., 1999). GFP targeted to the CC-ER provides an excellent system for studying the structure and dynamics of the ER within CCs and for the localization of promoter activity throughout the plant. As a comparison, in nontransgenic plants, the ER membrane can specifically be stained by $DiOC_6$ in living cells (Schulz, 1992; Terasaki and Reese, 1992).

Using confocal microscopy combined with fluorescence redistribution after photobleaching (FRAP) and two-photon microscopy, our goals were to (1) identify phloem regions active in Suc loading throughout the plant during development; (2) examine the live structure of CC-ER within functional SE-CC complexes; and (3) quantify membrane coupling between the CC-ER and SER in comparison with other tissues. Here we show that the ER membranes of CC and SE are intimately connected, providing a membrane pathway available for signal transduction and posttranslational membrane protein transport. However, GFP expressed within the ER lumen of CC did not traffic into SE, suggesting that the desmotubular lumen has a size exclusion limit smaller than 27 kD.

RESULTS

Activity of the *SUC2* Promoter

Transgenic tobacco expressing ER-targeted GFP under control of the CC-specific SUC2 promoter *AtSUC2* was used to identify those phloem regions involved in Suc loading. GFP expression was strong in the loading phloem of cotyledons and minor veins of source leaves, but was not restricted to these areas. According to the main function, phloem can be divided into collection phloem, transport phloem, and release phloem (van Bel, 2003). Table I summarizes data from different organs and developmental stages (see also Supplemental Fig. S1). GFP was found in all vein classes of source leaves and fully grown cotyledons. Dark-imbibed seeds were negative, whereas expression started in dark-germinated seedlings at the base of the cotyledons and in the hypocotyl 1 d after germination (Fig. 1A). In the cotyledon, GFP appeared

Table I. *SUC2 promoter activity in tobacco organs during development*

Tissue		Specific CC-ER-GFP Fluorescence
Adult plant	Source leaf	Internal and external phloem of all vein classes (I–VI). Lacking in class III over some distances near class II veins
	Transition leaf	Weak signal in CCs of internal and external phloem in midvein/petiole (class I)
	Sink leaf	Weak signal in CCs of external phloem in midvein/petiole (class I)
	Stem	Internal and external phloem in all developmental stages and in leaf traces
	Root	Phloem of the short tap root and adventitious roots
	Flower	In sepal and gynoecium phloem of flower buds, and after anthesis in petal, style, and stamen phloem as well
Seedling germinated in darkness (1 d after germination)	Cotyledons	Fluorescence develops acropetally in the midvein, then basipetally for the subsequent veins
	Roots	Phloem of the hypocotyl/root axis not beyond the root hair zone
Seed imbibed in darkness		None

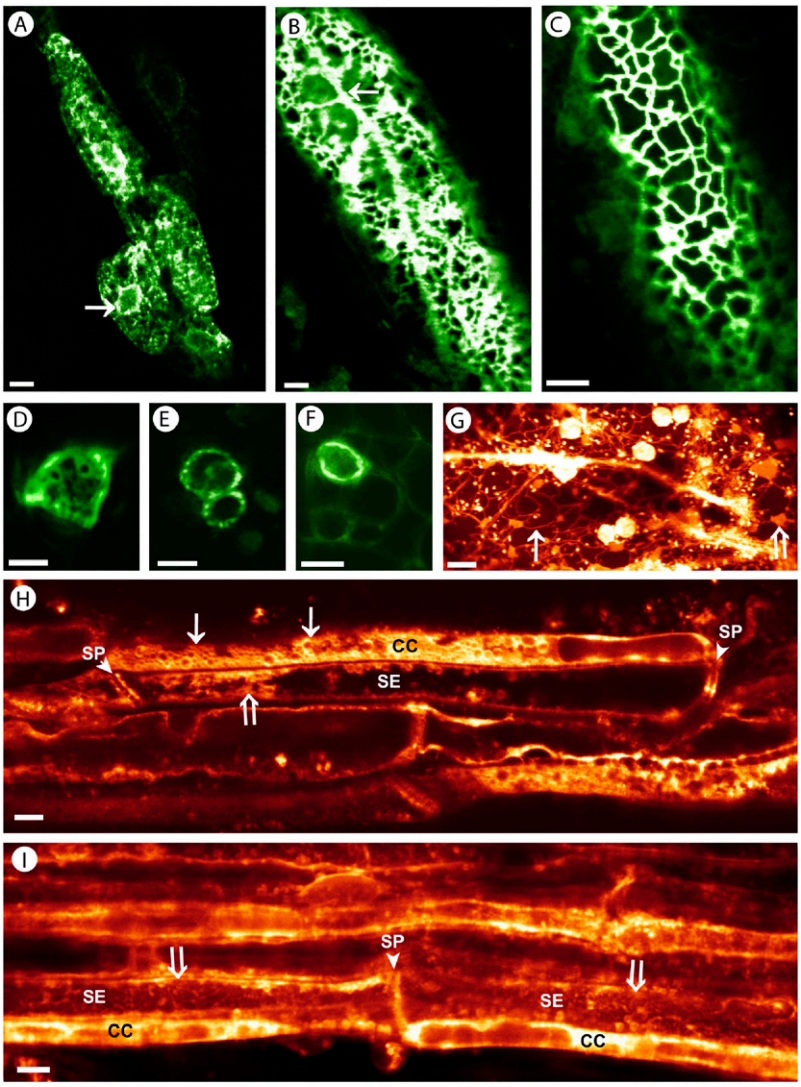

Figure 1. The dynamic structure of CC-ER in AtSUC2-GFP-ER tobacco (A–F) and in $DiOC_6$-stained tissue from wild-type plants (G–I). GFP fluorescence visualizes a cortical ER network in four CCs and the nuclear envelope (arrow) from the cotyledon of a 1-d-old, dark-grown seedling (A; detail from Supplemental Fig. S1C). Light-grown mature cotyledons show the same finely meshed network, underlined by longitudinal ER strands (arrow; B and C). Peripheral CC-ER fluorescence occurs in transport phloem throughout the plant as seen in cross sections of stem (D), petiole (E), and soil-grown lateral root (F). $DiOC_6$-stained vascular parenchyma with widely meshed cortical ER (arrow), longitudinal strands, and cisternal ER parts (white arrow) forms the background to vigorous cytoplasmic streaming of particles in the size of mitochondria (see Supplemental Movie S3). The large spherical organelles are autofluorescent chloroplasts (G). $DiOC_6$-stained stem phloem shows ER in all cell types. CCs identified by their ending at sieve plates (SP) exhibit cortical CC-ER network (arrows). SER lining the lateral wall and SPs have a diffuse tubular-to-vesicular structure as seen in glancing optical sections through the SE periphery (white arrows; H and I). Scale: A to E, 5 μm; F to I, 10 μm.

first in the midrib and subsequently in the other vein classes. In mature shoots and petioles, both the external and internal phloem were positive. Petioles and the midribs of the youngest unfolded leaves, defined as sink leaves, had GFP fluorescence in their CCs. The midribs stayed positive in the basal part of transition leaves throughout the sink-to-source transition. In nonphotosynthetic organs, GFP was seen in petals, styles, stamens, and roots (see Supplemental Fig. S1). Thus, the SUC2 promoter is active in the collection phloem as well as in the transport phloem. Only release phloem, such as that found in the second- and third-order veins in sink leaves and the unloading phloem of the root tip beyond the root-hair zone, was negative for GFP fluorescence (Table I).

CC-ER Structure and Dynamics

The structure and dynamics of the ER within CCs were studied in vivo in mature leaf segments and in whole detached leaves in ER-SUC2-GFP transformants, and also in $DiOC_6$-stained plants. Control experiments were performed on intact plants to ensure that any changes in subcellular structure were not caused by stress factors, such as preparative wounding. To obtain clear images, it was necessary to carefully remove the lower epidermis in the observed region. Figure 1 shows that the ER forms a cortical network in CCs of leaves (Fig. 1, A–C; see also Supplemental Movie S1), petioles, stems, and roots (Fig. 1, D–F). The cortical network is continuous with the nuclear envelope, which outlines the nuclei of CCs (Fig. 1A) and with tubular ER strands underlying the cortical network (Fig. 1B).

In contrast to GFP-expressing plants, $DiOC_6$-stained phloem depicted not only the CC-ER, but also the ER in neighboring cells, such as SEs and phloem parenchyma cells. Both the CC-ER as well as the ER in parenchyma cells formed a cortical network. The mesh width of the CC-ER was on average in the range of about 2 μm, whereas that of parenchyma cells was about 5 μm (compare Fig. 1, C and G). Parenchyma cells showed a vigorously streaming system of ER

tubules, cisternae, and small organelles in the size range of mitochondria. With the chosen filter settings, chloroplasts appear stained because of their chlorophyll autofluorescence (Fig. 1G; see Supplemental Movie S2). In SEs, $DiOC_6$-specific fluorescence lined the sieve plates as well as the lateral walls, but did not show a reticulate pattern. Glancing optical sections through the SE periphery revealed a more diffuse vesicular-to-tubular ER arrangement (Fig. 1, H and I).

Time-lapse movies of the cortical CC-ER showed the cortical network to be relatively immobile compared to the tubular ER within cells participating in cytoplasmic streaming. On a smaller scale, however, the network was intricate and showed constantly retracting and fusing ER elements (see Supplemental Movie S3).

ER Contact between SEs and CCs

To unequivocally identify SEs and their PPUs, tissue was stained with aniline blue, which labels callose and fluoresces yellow when excited with UV light. Live observations were hampered by the fact that the UV laser bleached the tissue strongly. Callose could, however, easily be visualized using two-photon excitation at 800 nm, which did not result in appreciable bleaching. At this wavelength, emission from GFP was very low and did not result in cross talk between the emission channels. Figure 2A shows the strongly labeled sieve plates of three sieve tubes (false-colored in blue) and the GFP florescence in three CCs. Lateral callose dots identify the PPUs in the common wall between SE and CC. Even with the most sensitive setting of the confocal laser-scanning microscope (CLSM), GFP fluorescence could not be detected on the SE side of the PPUs, indicating that the reporter protein is not able to escape the CC-ER via the desmotubule of the PPU (Fig. 2A).

In contrast, $DiOC_6$ staining of wild-type plants demonstrated that SEs do contain SER at their lateral walls and at the sieve plates (Figs. 1, H and I, and 2C). SEs were again identified by callose at sieve plates and PPUs. Colocalization of both dyes in the PPUs (Fig. 2B) might indicate that $DiOC_6$ also stains the ER component of PPUs. Comparison of CC-ER and SER at high magnification revealed a much larger amount of ER in the CC than in the SE and a faint fluorescence in the obliquely cut pits of the common wall (Fig. 2C, arrows).

ER Coupling as Revealed by Intercellular FRAP

The resolution limit of a CLSM does not allow an equivocal confirmation of continuity of the ER between CCs and SEs. Structural continuity can be resolved by electron microscopy. However, even if reconstruction of serial ultrathin sections gave evidence of a structural contact, this does not answer the question of whether the ER of both cell types has functional contact (i.e. whether membrane-associated molecules use this contact to traffic from the CC through the PPUs into the SE or vice versa).

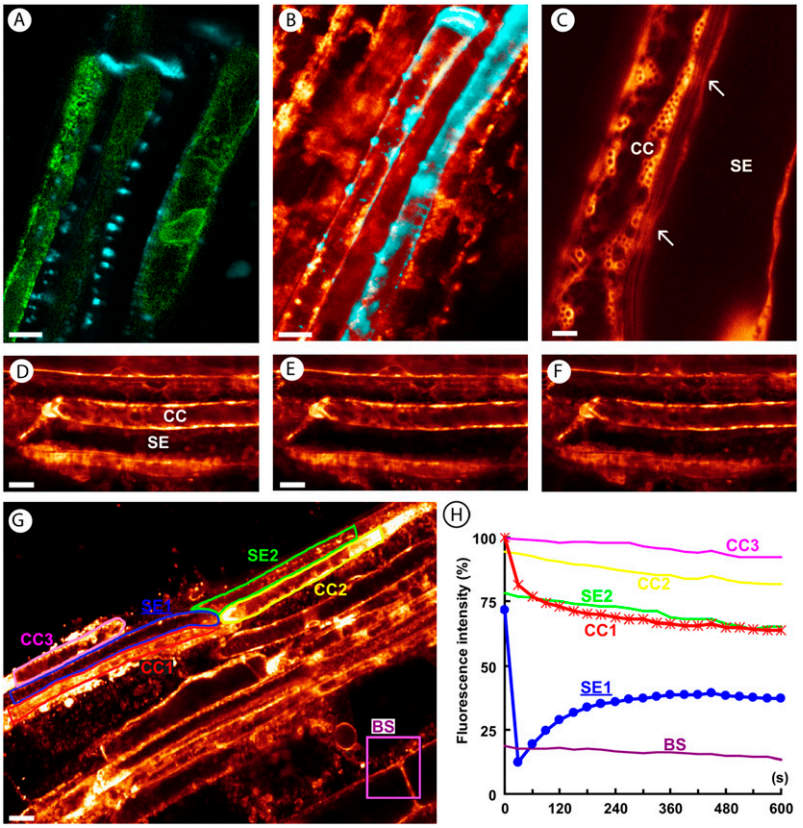

Figure 2. Contact between SEs and CCs as seen by confocal and two-photon microscopy (A–C) and measured by FRAP (D–H). Callose at sieve plates and PPUs is shown in blue by aniline blue staining of a SUC2-GFP-ER transformant (A) and of a $DiOC_6$-stained wild-type sample (B). GFP is not escaping the CCs (A). $DiOC_6$ is staining the ER of SEs, CCs, and phloem parenchyma cells. Colocalization of ER and callose at sieve plates and along the lateral SE walls is seen in white (B). High magnification of a SE and a CC, the latter of which with a cortical ER network. CC-ER and SER are close to each other at the arrows, possibly indicating PPUs (C). Coupling of CC-ER and SER is exemplified with images out of a FRAP series before bleaching (D), directly after bleaching (E), and 10 min later (F). G and H, In FRAP experiments, changes in the $DiOC_6$ fluorescence intensity were followed in the bleached SE (SE1) and its CC (CC1), in the next SE (SE2) and its CC (CC2), in an unrelated CC (CC3) and, as fading control, in a bundle sheath cell (BS; G). The chart is showing that loss of fluorescence in the bleached SE (circles) is accompanied by an immediate and drastic loss of fluorescence in the neighboring CC (stars) mirroring the redistribution of fluorescence into the SE. Fluorescence in the next SE and its CC declines linearly, parallel to CC1. The unrelated CC3 declines only slightly more than sample fading (H). Scale: A to F, 10 μm; G, 20 μm.

To answer this question, we used the FRAP technique. After staining the tissue with $DiOC_6$, large parts of SEs were bleached by illuminating them with full laser power. The redistribution of ER fluorescence was followed by time-lapse imaging. Figure 2, D to F, shows a SE before bleaching, immediately after bleaching, and 180 s later. Redistribution of $DiOC_6$ is indicated by the recovery of fluorescence at the sieve plate and the lateral walls of the SE.

For detailed analysis of dye movement in a phloem strand, experiments were standardized and the following regions of interest were selected for quantification (see Fig. 2G): In addition to the bleached part of the SE, fluorescence was measured beyond the sieve plate in the next SE, the sister CCs, and an unrelated CC. As a control for general fading during the recording period of 10 to 20 min, bundle sheath cells were selected. Figure 2H shows the time course of FRAP. Bleaching of part of a SE led to an immediate drop of fluorescence in the sister CC. This loss of fluorescence in the CC was accompanied by a corresponding gain in fluorescence within the bleached SE and followed an exponential time course. The next SE, its CC, and the unrelated CC showed a linear reduction in fluorescence over the observed time period. This reduction was larger than general fading, indicating a small contribution of these cells to FRAP (Fig. 2H).

The degree of ER coupling between cells has not been measured before in plant tissues. Therefore, we conducted FRAP studies with other tissues and compared the intercellular redistribution of $DiOC_6$ with intracellular redistribution along ER membranes. Figure 3 depicts examples of FRAP between spongy mesophyll cells and a guard cell pair (Fig. 3, C and D, respectively), showing a relatively slow redistribution of the dye. Bleaching only parts of the ER in a cell led to a much more rapid redistribution than when the entire cell was bleached (Fig. 3A), even when ER movements were eliminated by the actin inhibitor cytochalasin D (Fig. 3B). In the situation of intracellular bleaching, $DiOC_6$ does not have to cross plasmodesmata for redistribution. Intercellular FRAP could theoretically be biased by a contribution of apoplastic $DiOC_6$ that was not removed by the washing steps. However, this contribution could be excluded because bleaching of an entire stomatal complex (both cells of a guard cell pair) did not result in any fluorescence redistribution.

Comparison of the Degree of ER Coupling in Different Tissues

To compare ER coupling between cells in different tissues, two independent values were determined for each experiment, the half-life of redistribution ($T_{1/2}$) and

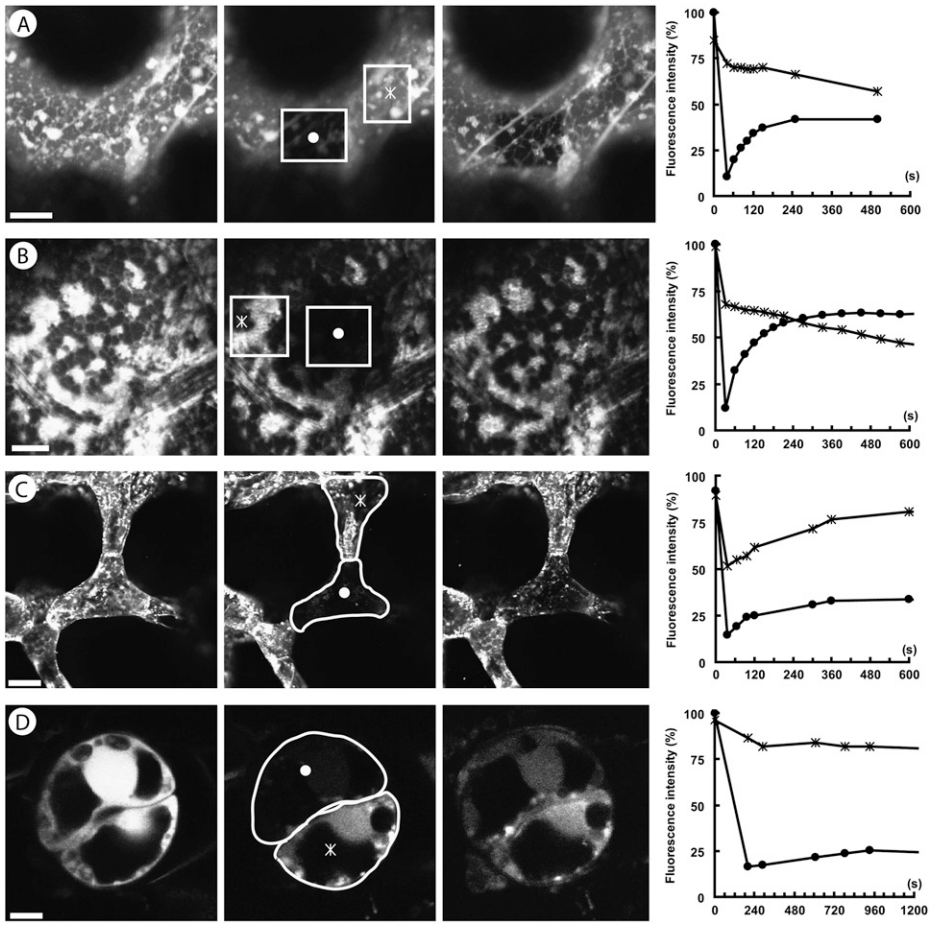

Figure 3. Intracellular FRAP (A and B) and intercellular FRAP (C and D) of ER in the epidermis (A), peduncle cortex parenchyma (B), leaf mesophyll (C), and guard cells (D). From left to right, each image shows cells before bleaching, directly after bleaching, and after the entire FRAP period, and a chart summarizing the observed changes in fluorescence. The bleached and neighboring regions measured for FRAP are indicated by a circle and a star, respectively. Photobleaching of a mesophyll cell results in redistribution from adjacent cells (C). For individual guard cells, the redistribution of fluorescence from its neighbor is very low (D). For intracellular FRAP, diffusion of dye into a bleached region is rapid as shown for an epidermis cell (A) and for cytochalasin D-treated parenchyma cells (B). Scale: A and B, 10 μm; C, 25 μm; D, 5 μm.

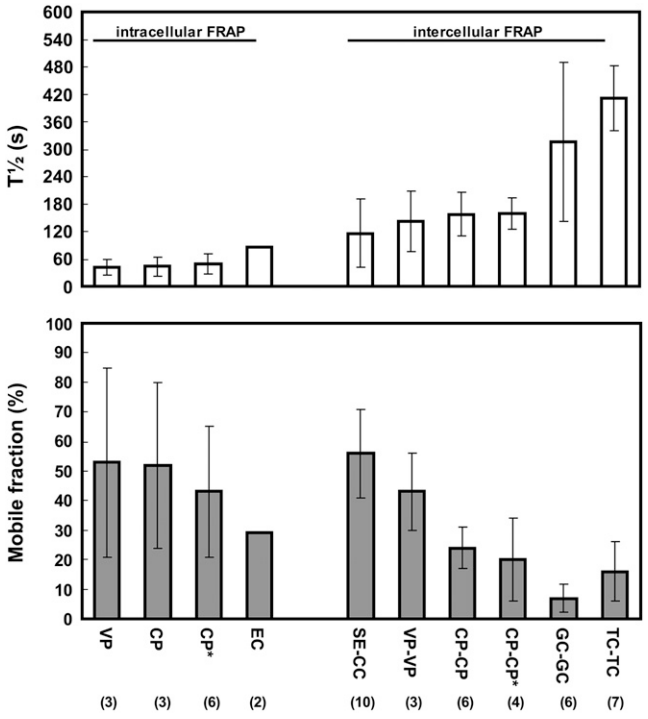

Figure 4. Quantification of intracellular and intercellular FRAP of $DiOC_6$-stained endomembranes within mature tobacco tissue. Half-life and mobile fraction of redistribution are indicated for vascular parenchyma cells (VP), cortex parenchyma cells (CP), and epidermis cells (EC) as well as between SE and CC, VP, CP, guard cells (GC), and trichome cells (TC), with the number of repetitions given in parentheses. Bars show SD. Intracellular FRAP is much more rapid than intercellular FRAP, whereas the mobile-fraction values are comparable. Best coupling is between SE and CC as demonstrated by a small half-life and a high mobile fraction. FRAP is slower between the other cell types and the mobile fraction is decreasing for vascular parenchyma cells, cortex parenchyma, and trichome cells, respectively. Guard cell pairs are coupled, but show the smallest mobile fraction of all cell types studied. No coupling could be measured between guard cells and surrounding epidermis cells. Cytochalasin D treatment (*) changed neither intracellular nor intercellular FRAP.

the mobile fraction, the latter indicating how much of the original fluorescence was recovered by redistribution of $DiOC_6$. Figure 4 summarizes the experiments and compares the values for intercellular FRAP with those of intracellular FRAP. From all cases of intercellular FRAP, the interface between SE and CC has the highest degree of coupling, followed by vascular parenchyma cells. A high degree of coupling is characterized by a large mobile fraction and a small half-life of FRAP (Fig. 4). Whereas the time course of redistribution is similar between different types of parenchyma tissue, the mobile fraction decreases considerably between vascular tissues and nonvascular tissues, being largest between CC and SE. The least degree of coupling was determined between sister guard cells of a stomatal complex and between trichome cells, showing a very long half-life and a small mobile fraction (Fig. 4). As expected, the ER of guard cells was isolated from the neighboring epidermis cells. Intracellular ER FRAP was about 2 to 3 times faster than intercellular FRAP, but showed a comparable percentage within the mobile fraction.

Effect of Cytoplasmic Streaming on FRAP

A possible contribution of cytoplasmic streaming to the redistribution of membrane constituents was excluded by incubating the tissue in the actin filament inhibitor cytochalasin D. Neither intracellular nor intercellular FRAP was influenced by this treatment (Fig. 4), whereas cytoplasmic streaming stopped within a few minutes. Interestingly, a circular shadow around the bleached area of the ER indicated that cytochalasin D treatment improved redistribution in the close vicinity of the bleached area, thus draining this area for $DiOC_6$ fluorescence (Fig. 3B).

DISCUSSION

The results achieved in this study using noninvasive bioimaging and the FRAP technique show clearly that SEs and CCs are intimately linked by the ER that traverses the PPU that connects these cell types. This observation has a number of implications for the transport of materials and signals between SEs and CCs.

Loading and Retrieval of Suc

The role of SUC2 (or other Suc proton symporters of the SUT 1 family; Kühn, 2003) in apoplasmic Suc loading into the collection phloem is undisputed and confirmed by the severe reduction in photoassimilate export from source leaves observed in *SUT1* antisense and knockout plants (Schulz et al., 1998; Gottwald et al., 2000). In this study, the reporter gene was expressed in the cotyledons of dark-grown seedlings, indicating that activation of the promoter is correlated with starch mobilization, but independent of light. This contrasts to shading experiments of sink-to-source transition leaves where light, or a product of light, was required for activation of the *SUC2* promoter in minor veins (Wright et al., 2003). It is conceivable that the promoter is activated by a certain level of Suc, which in cotyledons is supplied by starch mobilization and in transition leaves by photosynthesis. After partial shading, Suc in the shaded minor vein regions might not reach the critical concentration that is necessary to activate symporter expression (see discussion in Wright et al., 2003).

The *SUC2* promoter was not only active in collection phloem, but also in midribs of sink leaves, petioles, stems, roots, and flower organs (i.e. transport phloem). The function of the symporter cannot be limited to the uptake of Suc originating in residual photosynthesis in green petioles and stems, as shown by *SUC2* expression in roots and nonphotosynthetic flower organs. Rather, the expression pattern confirms that SUT1 family symporters are responsible for Suc retrieval along the transport phloem (Stadler and Sauer, 1996;

Eisenbarth and Weig, 2005). In sink leaves and sink regions of transition leaves, GFP expression was significant, but much weaker than in source regions. Therefore, in a previous publication using the same construct, it was not detected in the midribs of sink leaves (Wright et al., 2003). It can be concluded that *SUC2* is expressed throughout the transport phloem. Expression in dark-grown seedlings, in class II veins of shaded-leaf regions, and in roots demonstrates that activation of its promoter is light independent in transport phloem. It might be triggered by an increase in Suc concentration beyond a threshold value when an appreciable long-distance gradient develops. Suc retrieval might also be an inherent function of the SUC2 symporter in Arabidopsis (*Arabidopsis thaliana*) because ER-targeted and membrane-anchored GFP constructs were positive in light-grown roots (Stadler et al., 2005). However, light independence of the promoter for the transport phloem of Arabidopsis has yet to be tested.

Activity of the *SUC2* promoter in the transport phloem raises the questions of whether phloem transport and unloading of free GFP, expressed under the same promoter, really reflects long-distance transport or just results from local export out of the CCs in the transport phloem (Imlau et al., 1999; Wright et al., 2003). However, grafting experiments gave clear evidence that free GFP is indeed traveling with the phloem sap from source to sink (Imlau et al., 1999). In ungrafted plants, the free GFP translocated and unloaded in sink tissues might include a minor amount of GFP originating in the transport phloem en route. This does not change the significance of the GFP transport results for phloem transport and unloading.

Experimental evidence is accumulating to confirm the significance of Suc retrieval for phloem function (Ayre et al., 2003). Inhibition of retrieval by locally applied hypoxic conditions leads to a reduction of both the concentration and the transport rate of Suc in the phloem (van Dongen et al., 2003). Recently, direct measurements showed that transport phloem SEs produce a membrane potential sufficient to outcompete phloem parenchyma in photosynthate acquisition from the apoplast (Hafke et al., 2005). It can be concluded that Suc symporters in the transport phloem are important for retrieving leaked Suc from the apoplast. Under certain conditions, symporters might even work as release carriers (e.g. to supply a lateral sink, as patch clamp studies of the ZmSUT1 symporter have indicated; Carpaneto et al., 2005). This option seems, however, not to be realized in developing organs.

The root tip below the root hair zone, the second- and third-class veins of sink leaves of tobacco (this study; Wright et al., 2003), and the elongating hypocotyls of etiolated Ricinus seedlings (Eisenbarth and Weig, 2005) are devoid of Suc symporter activity as evidenced by reporter gene expression and immunolocalization, respectively. This indicates that retrieval of Suc stops in the release phloem, independent of the mode of unloading. Unloading in sink leaves and at root tips is generally symplasmic (Ding et al., 1988; Roberts et al., 1997; Schulz, 2005), whereas it might be apoplasmic in the elongating hypocotyls of Ricinus (Eisenbarth and Weig, 2005).

Function of Cortical ER in CCs

CCs are characterized by electron-dense cytoplasm in the electron microscope (Evert, 1990), which hides the organization of the ER (see Wooding and Northcote, 1965). Using confocal microscopy, this study depicted a prominent, finely meshed cortical ER network (mesh width about 1–3 μm), both in transformants where GFP was targeted to the CC-ER and in $DiOC_6$-stained wild-type plants (Fig. 1). Phloem parenchyma cells also showed a cortical ER network that was more mobile than that of the CCs and had a larger mesh width. Noncortical ER participated vigorously in cytoplasmic streaming. A relatively stationary cortical ER network and a vigorously streaming inner ER have already been described for onion (*Allium cepa*) bulb epidermal cells (Knebel et al., 1990). A cortical ER network with meshes of 5- to 10-μm width is characteristic of epidermal cells and is held in place by an underlying network of actin filaments (Quader et al., 1989; Boevink et al., 1998). Cytoplasmic streaming, as well as rearrangement of this network, is dependent upon the actin-myosin system, as seen by the effects of cytochalasin D treatment (this study; Knebel et al., 1990). The ER network in CCs, shown here, is more regularly spaced and has a much smaller mesh width than epidermal cells.

Although much is known about the nature and function of plant ER, including lipid renewal and exchange with other organelles or the plasma membrane (Staehelin, 1997; Voeltz et al., 2002), the role of the cortical network observed in different cell types remains to be determined. In tobacco epidermis cells, the cortical ER network was shown to interact with the Golgi and to be involved in the retrograde transport of malfolded proteins back into the cytosol with reporter gene constructs (Brandizzi et al., 2002, 2003). Using photoactivated GFP, Runions and coworkers (2005) demonstrated that membrane proteins move more rapidly in the ER than can be explained by simple diffusion. A reticulate subdomain of the ER seems to be involved in the transfer of ascorbate peroxidase to peroxisomes (Mullen et al., 1999). It is, however, not clear whether these functions are limited to the cortical network, where they might be more easily visualized, or whether they occur throughout the ER compartment.

A fine cortical network in animal egg cells was found to have an important function in the propagation of calcium waves at fertilization. It contains inositol 1,4,5-phosphate receptors involved in sperm-induced Ca^{2+} transients (Kline et al., 1999). Thus, cortical ER acts as a pacemaker site dedicated to the initiation of global calcium waves in the highly polarized egg cell (Dumollard et al., 2002). Considering the importance of a sudden increase in the cytosolic calcium for callose

synthesis at plasmodesmata and sieve pores (Kauss, 1985; Verma and Hong, 2001), the elaborate ER network in CCs might as well act as a pacemaker for calcium waves in the SE-CC complex following wounding or pathogen attack.

ER Coupling of SEs and CCs

The ER compartment can be divided into as many as 16 functional domains, but its lumen is continuous throughout the cell, including the nuclear envelope (Staehelin, 1997; Nehls et al., 2000). Microinjection of fluorochromes into the ER of epidermal cells revealed that this compartment may be continuous with the ER of neighboring cells. Fluorochromes of up to 10,000 D were observed to move into cells neighboring the injected one (Cantrill et al., 1999). Considering the specific rod-like structure and proteinaceous nature of the desmotubule, lumenal continuity does not necessarily mean that the ER membranes of neighboring cells are continuous. Microinjection into the ER of CCs would be extremely difficult and would change the physiology of these cells considerably. In this study, SEs were studied with high resolution and sensitivity using GFP targeted to the ER of CCs. Failure to detect GFP fluorescence in SEs of SUC2-ER GFP-expressing plants confirms earlier results (Wright et al., 2003) and can be due to a discontinuity of CC-ER and SER at this specific interface, or possibly to a lumenal size exclusion limit at the PPUs below the Stokes radius of GFP (1.8 nm).

Using the ER-specific $DiOC_6$ and selective bleaching of the SER, we could demonstrate redistribution of the fluorochrome and thus continuity of ER between CC and SE. Because bleaching of fluorochromes is an irreversible process, new fluorescence in the bleached cell must come from outside the bleached region, either from within the same cell or from neighboring cells. FRAP indicates that membrane lipids can be exchanged across the PPU. The degree of intercellular ER coupling is dependent on many parameters, such as the number of plasmodesmata per shared interface, dimensions of the desmotubules, and the degree of contact between desmotubules and the tubular and cisternal components of the ER. The half-life and mobile-fraction values of FRAP experiments can be integrated over all these parameters and give a simple measure of ER coupling in different tissues. To date, only Grabski et al. (1993) quantified the degree of ER coupling between suspension culture cells of soybean (*Glycine max*). The time range of intercellular and intracellular fluorochrome redistribution documented for suspension culture cells was in the same range as these results (i.e. about 20 and 3 min, respectively). $DiOC_6$ is known to stain the ER and mitochondria (Terasaki and Reese, 1992). Any unspecific staining of the plasma membrane would bias the results of this study because the dye could redistribute via the plasmodesmal plasma membrane as an alternative pathway. With the chosen dye concentration, unspecific staining is, however, improbable (see Waterman-Storer and Simon, 1998). Moreover, a study on Hechtian strands gave evidence that the plasma membrane of tobacco cells is negative for $DiOC_6$ staining because some of the observed Hechtian strands did not contain a stainable compound. Hechtian strands consist of a plasma membrane tubule, which may or may not enclose the ER (Buer et al., 2000).

FRAP theory primarily deals with determining diffusion coefficients from short-term bleaching of a small spot in a planar, uniform membrane (Weiss, 2004). Thus, in most live cell experiments dealing with complex three-dimensional cells, FRAP studies are a simplification that does not account for membrane geometry. Moreover, planar models for membrane redistribution are not valid for plasmodesmata, which form the rate-limiting step in intercellular exchange of membrane-associated molecules. In our study, the mobile fraction, which indicates how much of the fluorochrome is available for redistribution, is likely to be underestimated because we did not correct for general background fading.

Comparison of FRAP in different tissues showed that the most intimate ER coupling occurs between SE and CC and between adjoining vascular parenchyma cells (Fig. 4). The half-life of redistribution increases and the mobile fraction decreases, for cortex parenchyma, trichomes, and guard cells, respectively. The ER of mature guard cells is not coupled to neighboring cells, correlated with the loss of functional plasmodesmata at this interface (Wille and Lucas, 1984). Cytochalasin D, an inhibitor of actin polymerization, did not change the degree of ER coupling, indicating that transport of lipophilic substances in the ER and desmotubules does not require actin-driven flow (see membrane protein movement; Runions et al., 2005).

The intimate coupling of ER between CC and SE provides a pathway for molecular trafficking into the SE, which is undisturbed by the rapid stream of solutes passing through the SE lumen. It can be assumed that the exchange of membrane components, including ER-trafficked proteins, is essential for the integrity of the SE plasma membrane for as long as the SE remains functional. The possibility of membrane trafficking from CCs into SEs is represented by the rapid redistribution of the lipophilic dye $DiOC_6$ in this study.

This study does not provide evidence for intralumenal protein coupling between CCs and SEs, although it might be expected that small ions, such as calcium, may pass, considering the desmotubular size exclusion limit shown by Cantrill et al. (1999) between adjoining epidermal cells. If this were the case, the lumen of the SER might be considered as an extension of the calcium store of CCs. Besides a possible role in initiating the callose reaction in individual SEs, it is attractive to speculate that the SER may be involved in creating and maintaining calcium waves through the sieve-tube system for long-distance signaling, wound, and pathogen responses (van Bel and Ehlers, 2005). In this long-distance signaling system, CCs may act as relay stations to reenhance signals that apparently proceed more rapidly than solute transport.

CONCLUSION

In this study, we report that the CC-specific *SUC2* promoter is active not only in the collection phloem of tobacco transformants, but also in all regions of the transport phloem, including midveins of sink leaves, nonphotosynthetic organs such as roots and flowers, and very young seedlings. GFP targeted to the ER lumen remained in CCs and was not detected in SEs. However, the ER membrane is functionally continuous between CCs and SEs as demonstrated by FRAP of $DiOC_6$-stained phloem. Physical continuity of the ER, but lack of lumenal GFP transfer, indicates that the desmotubules of the PPUs have a size exclusion limit below 27 kD. The specialized plasmodesmata (PPUs) that connect CCs and SEs, which have a particularly large size exclusion limit for phloem-derived proteins (Stadler et al., 2005), are also shown here to also offer an intimate ER contact that allows a high exchange rate of ER-associated molecules compared to other cell types.

MATERIALS AND METHODS

Plant Material

Transgenic tobacco (*Nicotiana tabacum*) expressing GFP under the control of the CC-specific promoter *AtSUC2* (Imlau et al., 1999) was further added to an ER-targeting sequence (mGFP5-ER) and a HDEL ER retention sequence as described in Wright et al. (2003), thus expressing CC-specific, ER-localized GFP. This transgenic line and nontransgenic tobacco cv Samsun were grown from seed in a greenhouse throughout the year under additional artificial daylight (16/8-h photoperiod at 135 μmol m^{-2} s^{-1} photosynthetically active radiation) and temperature control (minimal 25°C d/17°C night). Embryos were prepared from seeds germinated in darkness on wet filter paper.

Preparation and Staining of Plant Material

All unfolded leaves of approximately 30-cm high transgenic tobacco plants were studied for GFP expression. Whole sink leaves (maximal 15 mm in length), segments (2 × 2 cm) of transition and source leaves, and petiole, stem, root, peduncle, sepal, petal, stamen, and style sections from transgenic tobacco were mounted in distilled water on microscope slides. For the purpose of this study, sink leaves were defined as being the youngest unfolded leaves and smaller than 15 mm in length. In a previous publication using the same construct, leaves up to 50 mm in length were shown by unloading of free GFP to be entirely sink (Wright et al., 2003). Transition leaves were defined as leaves showing ER-localized GFP in the minor veins of the leaf tip, and source leaves were defined as having ER-localized GFP in the minor veins throughout the leaf. Embryos were prepared from seed under a dissection microscope and immobilized with a spray adhesive (Medical Adhesive) on a microscope slide and mounted in water. Nontransgenic tobacco was incubated in 2 μg/mL $DiOC_6$ (Molecular Probes) for 10 min at room temperature and rinsed three times in distilled water for removal of extracellular fluorochrome. For the stock solution, 2 mg $DiOC_6$ were dissolved in less than 5 μL dimethyl sulfoxide and diluted to 2 mg/mL with distilled water. To get clear images of the leaf minor vein system, the abaxial epidermis was removed within a small area. Callose in the sieve plates and sieve areas of SEs was detected with 0.01% (w/v) aniline blue (Merck) in 0.1 M phosphate buffer, pH 7.4.

For whole-plant experiments, $DiOC_6$ was infiltrated through stomata on an abaxial leaf epidermis using a syringe without a needle. The leaf part was then attached to an object slide using a spray adhesive and, after peeling off a small area of epidermis, the structure and dynamics of ER were examined with a dipping lens and compared to detached leaf samples. Similar setups were used to examine the ER-GFP in intact plants.

Confocal and Two-Photon Microscopy

A two-photon CLSM (Leica TCS SP2/MP; Leica Microsystems) equipped with UV, visible, and pulsed infrared lasers was used. GFP expression was imaged using the 488-nm argon laser for excitation and an emission range of 505 to 525 nm. $DiOC_6$-stained material was excited with a 488-nm laser and emission was recorded at 503 to 523. Aniline blue can be excited with the 351- and 364-nm UV laser and emission recorded at 450 to 510 nm. However, to avoid bleaching observed with UV excitation, the fluorochromes were excited by the two-photon technique at 800 nm instead. When aniline blue was viewed together with one of the other dyes, the images were recorded by sequential scanning of frames.

FRAP

The mobility of the lipophilic $DiOC_6$ molecules in the ER was visualized and quantified using FRAP (see Ward and Brandizzi, 2004). The cells were loaded as described above. FRAP in the ER was performed within regions of interest using rapid switching between low-intensity imaging (488 nm) and a high-intensity bleach mode (488 nm) in various tissues. A prebleach image was collected using a 20× water objective lens (unidirectional scan, 26% laser intensity, zoom 4×, resolution 1,024 × 1,024, line average 2) in an area in which the ER membrane was in focus in several neighboring cells. A whole cell was selected and its fluorescence was photobleached during 20 bidirectional scans (100% laser intensity, zoom 16×, resolution 1,024 × 1,024, line average 2). The settings were quickly changed back to low-intensity imaging and a series of postbleaching scans were performed with the same settings as the prebleaching scans. The postbleach fluorescence was sampled every 30 s for 200 s followed by sampling every 60 s for 900 s, altogether approximately 18 min.

Provided that the bleached cell is connected to its adjacent unbleached neighbors by permeable plasmodesmata, an increase in fluorescence intensity is observed and recorded in the bleached cell. The FRAP curve gives two independent parameters: the mobile fraction M (the degree in percent to which the final fluorescence approaches the prebleach value, $M = [(F_\infty - F_0)\cdot 1/(F_{pre} - F_0)]\cdot 100\%$ and $T_{½}$ (time at which fluorescence reaches 50% of a plateau of intensity). The data were not adjusted for sample fading during the experiment, but for each analysis at least two background intensities were determined. Typically, background fading was between 1% to 2% fluorescence intensity per 15 min. Intracellular diffusion of dye was measured within vascular parenchyma and peduncle cortex parenchyma. Unlike the cell-to-cell experiments, intracellular FRAP was performed by bleaching only part of the cell using 10 bidirectional scans and recording a postbleach series for 10 min.

Inhibition of Cytoplasmic Streaming by an Actin Inhibitor

In some experiments, $DiOC_6$-stained samples were incubated for 5 min at room temperature in 1 μg/mL concentration of cytochalasin D (Sigma Chemical Company; obtained from *Zygosporium monsoni*) and imaged in a drop of the drug. A 1-mg/mL stock solution was made by dissolving 1 mg cytochalasin D in less than 5 μL dimethyl sulfoxide and diluted in 1 mL.

Supplemental Data

The following materials are available in the online version of this article.

Supplemental Figure S1. Confocal micrographs from tobacco expressing ER-targeted GFP under the Arabidopsis *SUC2* promoter.

Supplemental Movie S1. Cortical ER network in CCs from AtSUC2-ER-GFP tobacco (3-D stack).

Supplemental Movie S2. Time-lapse movie showing the dynamics of CC-ER from AtSUC2-ER-GFP tobacco. Images were captured every 12 s.

Supplemental Movie S3. Time-lapse movie showing the dynamics of phloem parenchyma from wild-type tobacco stained with $DiOC_6$. Images were captured every 5 s.

Received June 26, 2006; accepted August 7, 2006; published August 11, 2006.

LITERATURE CITED

Ayre BG, Keller F, Turgeon R (2003) Symplastic continuity between companion cells and the translocation stream: long-distance transport

is controlled by retention and retrieval mechanisms in the phloem. Plant Physiol **131:** 1518–1528

Boevink P, Oparka K, Santa Cruz S, Martin B, Betteridge A, Hawes C (1998) Stacks on tracks: the plant Golgi apparatus traffics on an actin/ER network. Plant J **15:** 441–447

Brandizzi F, Hanton S, DaSilva LLP, Boevink P, Evans D, Oparka K, Denecke J, Hawes C (2003) ER quality control can lead to retrograde transport from the ER lumen to the cytosol and the nucleoplasm in plants. Plant J **34:** 269–281

Brandizzi F, Snapp E, Roberts AG, Lippincott-Schwartz J, Hawes C (2002) Membrane protein transport between the endoplasmic reticulum and the Golgi in tobacco leaves is energy dependent but cytoskeleton independent: evidence from selective photobleaching. Plant Cell **14:** 1293–1309

Buer CS, Weathers PJ, Swartzlander GA Jr (2000) Changes in Hechtian strands in cold-hardened cells measured by optical microsurgery. Plant Physiol **122:** 1365–1378

Cantrill LC, Overall RL, Goodwin PB (1999) Cell-to-cell communication via plant endomembranes. Cell Biol Int **23:** 653–661

Carpaneto A, Geiger D, Bamberg E, Sauer N, Fromm J, Hedrich R (2005) Phloem-localized, proton-coupled sucrose carrier ZmSUT1 mediates sucrose efflux under the control of the sucrose gradient and the proton motive force. J Biol Chem **280:** 21437–21443

Crawford KM, Zambryski PC (2000) Subcellular localization determines the availability of non-targeted proteins to plasmodesmatal transport. Curr Biol **10:** 1032–1040

Ding B, Parthasarathy MV, Niklas K, Turgeon R (1988) A morphometric analysis of the phloem-unloading pathway in developing tobacco leaves. Planta **176:** 307–318

Dumollard R, Carroll J, Dupont G, Sardet C (2002) Calcium wave pacemakers in eggs. J Cell Sci **115:** 3557–3564

Eisenbarth DA, Weig AR (2005) Sucrose carrier RcSCR1 is involved in sucrose retrieval, but not in sucrose unloading in growing hypocotyls of *Ricinus communis* L. Plant Biol **7:** 98–103

Evert RF (1990) Dicotyledons. *In* H-D Behnke, RD Sjolund, eds, Sieve Elements—Comparative Structure, Induction and Development. Springer-Verlag, Berlin, pp 103–137

Gottwald JR, Krysan PJ, Young JC, Evert RF, Sussmann MR (2000) Genetic evidence for the in planta role of phloem-specific plasma membrane sucrose transporters. Proc Natl Acad Sci USA **97:** 13979–13984

Grabski S, de Feijter AW, Schindler M (1993) Endoplasmic reticulum forms a dynamic continuum for lipid diffusion between contiguous soybean root cells. Plant Cell **5:** 25–38

Hafke JB, van Amerongen J-K, Kelling F, Furch ACU, Gaupels F, van Bel AJE (2005) Thermodynamic battle for photosynthate acquisition between sieve tubes and adjoining parenchyma in transport phloem. Plant Physiol **138:** 1527–1537

Imlau A, Truernit E, Sauer N (1999) Cell-to-cell and long-distance trafficking of the green fluorescent protein in the phloem and symplastic unloading of the protein into sink tissues. Plant Cell **11:** 309–322

Kauss H (1985) Callose biosynthesis as a Ca^{2+}-regulated process and possible relations to other metabolic changes. J Cell Sci Suppl **2:** 89–103

Kline D, Mehlmann L, Fox C, Terasaki M (1999) The cortical endoplasmic reticulum (ER) of the mouse egg: localization of ER clusters in relation to the generation of repetitive calcium waves. Dev Biol **215:** 431–442

Knebel W, Quader H, Schnepf E (1990) Mobile and immobile endoplasmic reticulum in onion bulb scale epidermis: short- and long-term observations with a confocal laser scanning microscope. Eur J Cell Biol **52:** 328–340

Kühn C (2003) A comparison of the sucrose transporter systems of different plant species. Plant Biol **5:** 215–232

Kühn C, Franceschi VR, Schulz A, Lemoine R, Frommer WB (1997) Macromolecular trafficking indicated by localization and turnover of sucrose transporters in enucleate sieve elements. Science **275:** 1298–1300

Lazzaro MD, Thomson WW (1996) The vacuolar tubular continuum of living trichomes of chickpea (*Cicer arietinum*) provides a rapid means of solute delivery from base to tip. Protoplasma **193:** 181–190

Mullen RT, Lisenbee CS, Miernyk JA, Trelease RN (1999) Peroxisomal membrane ascorbate peroxidase is sorted to a membranous network that resembles a subdomain of the endoplasmic reticulum. Plant Cell **11:** 2167–2185

Nehls S, Snapp EL, Cole NB, Zaal KJ, Kenworthy AK, Roberts TH, Ellenberg J, Presley JF, Siggia E, Lippincott-Schwartz E (2000) Dynamics and retention of misfolded proteins in native ER membranes. Nat Cell Biol **2:** 288–295

Oparka KJ, Turgeon R (1999) Sieve elements and companion cells—traffic control centers of the phloem. Plant Cell **11:** 739–750

Quader H, Hofmann A, Schnepf E (1989) Reorganization of the endoplasmic reticulum in epidermal cells of onion bulb scales after cold stress: involvement of cytoskeletal elements. Planta **177:** 273–280

Roberts AG (2005) Plasmodesmal structure and development. *In* KJ Oparka, ed, Plasmodesmata. Annual Plant Reviews, Vol 18. Blackwell Scientific Publications, Oxford, pp 1–32

Roberts AG, Santa Cruz S, Roberts IM, Prior DAM, Turgeon R, Oparka KJ (1997) Phloem unloading in sink leaves of *Nicotiana benthamiana*: comparison of a fluorescent solute with a fluorescent virus. Plant Cell **9:** 1381–1396

Runions J, Brach T, Kühner S, Hawes C (2005) Photoactivation of GFP reveals protein dynamics within the endoplasmic reticulum membrane. J Exp Bot **57:** 43–50

Schulz A (1992) Living sieve cells of conifers as visualized by confocal, laser-scanning fluorescence microscopy. Protoplasma **166:** 153–164

Schulz A (1998) The phloem: structure related to function. Prog Bot **59:** 429–475

Schulz A (1999) Physiological control of plasmodesmal gating. *In* AJE van Bel, WJP van Kesteren, eds, Plasmodesmata. Structure, Function, Role in Cell Communication. Springer-Verlag, Berlin, pp 173–204

Schulz A (2005) Role of plasmodesmata in solute loading and unloading. *In* KJ Oparka, ed, Plasmodesmata. Annual Plant Reviews, Vol 18. Blackwell Scientific Publications, Oxford, pp 135–161

Schulz A, Kühn C, Riesmeier JW, Frommer WB (1998) Ultrastructural effects in potato leaves due to antisense-inhibition of the sucrose transporter indicate an apoplasmic mode of phloem loading. Planta **206:** 533–543

Sjölund RD (1997) The phloem sieve element: a river runs through it. Plant Cell **9:** 1137–1146

Sjolund RD, Shih CY (1983) Freeze-fracture analysis of phloem structure in plant tissue cultures. I. The sieve element reticulum. J Ultrastruct Res **82:** 111–121

Stadler R, Sauer N (1996) The *Arabidopsis thaliana AtSUC2* gene is specifically expressed in companion cells. Bot Acta **109:** 261–340

Stadler R, Wright KM, Lauterbach C, Amon G, Gahrtz M, Feuerstein A, Oparka KJ, Sauer N (2005) Expression of GFP-fusions in Arabidopsis companion cells reveals non-specific protein trafficking into sieve elements and identifies a novel post-phloem domain in roots. Plant J **41:** 319–331

Staehelin LA (1997) The plant ER: a dynamic organelle composed of a large number of discrete functional domains. Plant J **11:** 1151–1165

Terasaki M, Reese TS (1992) Characterization of endoplasmic reticulum by co-localization of BiP and dicarbocyanine dyes. J Cell Sci **101:** 315–322

van Bel AJE (2003) The phloem, a miracle of ingenuity. Plant Cell Environ **26:** 125–149

van Bel AJE, Ehlers K (2005) Electrical signalling via plasmodesmata. *In* KJ Oparka, ed, Plasmodesmata. Annual Plant Reviews, Vol 18. Blackwell Scientific Publications, Oxford, pp 263–278

van Bel AJE, van Rijen HVM (1994) Microelectrode-recorded development of the symplasmic autonomy of the sieve element/companion cell complex in the stem phloem of *Lupinus luteus* L. Planta **192:** 165–175

van Dongen JT, Schurr U, Pfister M, Geigenberger P (2003) Phloem metabolism and function have to cope with low internal oxygen. Plant Physiol **131:** 1529–1543

Verma DP, Hong Z (2001) Plant callose synthase complexes. Plant Mol Biol **47:** 693–701

Voeltz GK, Rolls MM, Rapoport TA (2002) Structural organization of the endoplasmic reticulum. EMBO Rep **3:** 944–950

Ward TH, Brandizzi F (2004) Dynamics of proteins in Golgi membranes: comparisons between mammalian and plant cells highlighted by photobleaching techniques. Cellul Mol Life Sci **61:** 172–185

Waterman-Storer CM, Simon ED (1998) Endoplasmic reticulum membrane tubules are distributed by microtubules in living cells using three distinct mechanisms. Curr Biol **8:** 798–806

Weiss M (2004) Challenges and artifacts in quantitative photobleaching. Traffic **5:** 662–671

Wille AC, Lucas WJ (1984) Ultrastructural and histochemical studies on guard cells. Planta **160:** 129–142

Wooding FBP, Northcote DH (1965) The fine structure and development of the companion cell of the phloem of *Acer pseudoplatanus*. J Cell Biol **24:** 117–128

Wright KM, Roberts AG, Martens HJ, Sauer N, Oparka KJ (2003) Structural and functional vein maturation in developing tobacco leaves in relation to *ATSUC2* promoter activity. Plant Physiol **131:** 1555–1565